International Journal of GEOMATE, April, 2020, Vol.18, Issue 68, pp. 21- 28
ISSN: 2186-2982 (P), 2186-2990 (O), Japan, DOI: https://doi.org/10.21660/2020.68.5582
Special Issue on Science, Engineering and Environment

LABORATORY EXPERIMENT OF CHANNEL HEAD BIFURCATION BY RADIAL OVERLAND FLOW

*Adichai Pornprommin[1], Ravicha Thaisiam[1] and Wandee Thaisiam[1]

[1]Department of Water Resources Engineering, Faculty of Engineering, Kasetsart University, Thailand

*Corresponding Author, Received: 14 June 2019, Revised: 08 Nov. 2019, Accepted: 12 Feb. 2020

ABSTRACT: Many studies have shown that incipient channelization can be explained by the interaction between flow and an erodible bed. Our recent theoretical study has shown that an eroding channel head by overland flow can maintain its shape without bifurcation if the flow depth is sufficiently large comparing to the channel head radius. Here, we performed nine experimental runs using three sediment sizes to provide better understanding of the bifurcation. A circular pan was filled with sand except at the center, where there were a sink hole and a drain installed at the pan bottom. When water had been filled over the sand to a desirable level, the drain was opened and unsteady radial overland flow accelerated toward the hole. After a while, water formed a downward-concave profile, leading to strong bed erosion in the vicinity of the hole and, as a result, the hole size expanded. In the initial development where flow depth was sufficiently large, the hole maintained its circular shape without channel incision while expanding. As the flow depth and discharge reduced and the hole radius increased, the hole started to lose its circular shape. Thus, the experimental results confirmed the condition of channel bifurcation proposed by our previous study. Main incised channels with large spacing were firstly initiated and elongated upstream in the radial direction while small rills were generated later between main channels. Using the network circularity as an indicator, we propose the new four phases of channel network development (unchannelization, initiation, extension and abstraction).

Keywords: Erosion, Channel head bifurcation, Overland flow, Experiment, Channel network development

1. INTRODUCTION

Channel head bifurcation, sometimes called branching, is one of the most important processes of channel network formation because it leads to a higher complexity in the geometry of the channel networks. Recently, researchers have tried to study its mechanics. Perron et al. [1] investigated the branching river networks of two field sites, the Allegheny Plateau in Pennsylvania and Gabilan Mesa in California. Using the landscape evolution model based on soil creep and channel incision equations, they found good agreement between their model and the field data. Using a groundwater flow equation, Petroff et al. [2] studied stream bifurcation by seepage. They compared their model with field observation at the Panhandle in Florida and found good agreement between them. Thus, both studies showed that channel head bifurcation should be initiated by hydrophysical mechanisms (processes due to water forces such as erosion), not as a consequence of random topology. Pornprommin et al. [3] performed a linear stability analysis using the flow equations in the polar coordination system to investigate incipient channel head bifurcation. Circular holes were assumed to be channel heads, toward which radial overland flow accelerates. Then, channel bifurcation is defined as the holes lose their circular shapes when they are unstable to the imposed perturbations. They estimated that channel head does not bifurcate if channel head radius is not larger than approximately 10 times the Froude-critical depth of overland flow divided by the friction coefficient [3].

A few experiments have been conducted to investigate the development of the channel head. Pornprommin et al. [4] performed an experiment of channel inception by seepage erosion on a rectangular basin with an adjustable bed slope. The sediment layer was built by coarse sand and water was fed upstream. They found that an increase in the slope led to a larger channel width but more difficulty in channel bifurcation. A higher discharge also caused a larger channel width but easier initiation of the bifurcation. Thus, they hypothesized that the geometry of groundwater flow and the resistibility of sediment material to slope failure play an important role in channel head bifurcation. Berhanu et al. [5] studied channel head shapes in a rectangular box filled with glass beads. Groundwater was fed by an upstream reservoir or rain. They found that the different sources of groundwater led to change in the groundwater flow nets and, consequently, impacted the shape of the channel heads. Their finding was consistent with the hypothesis of Pornprommin et al. [4]. A more comprehensive experiment of channel formation by seepage due to different groundwater flow patterns was conducted by [6]. However, to the authors' knowledge no experimental studies have tried to

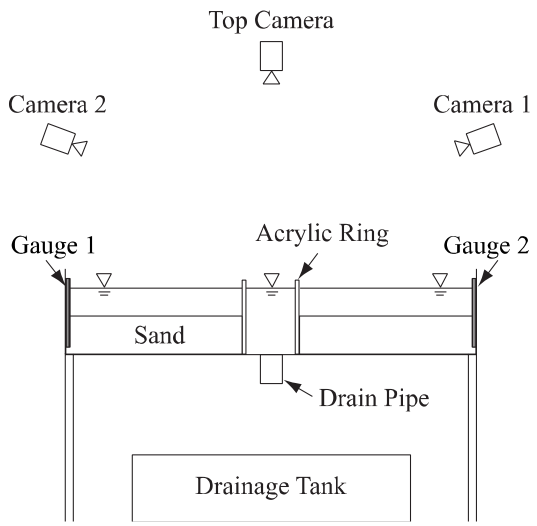

Fig. 1 Experiment setup.

investigate channel head bifurcation from the perspective of surface sheet flow in detail.

In this paper, we conducted a laboratory experiment of channel inception by overland flow in a circular chamber following the concept of channel bifurcation proposed by [3]. Our two main objectives in this study were; (i) to examine the early stage of channel network evolution (channel inception); and (ii) to compare the experimental results with the theoretical study [3].

2. EXPERIMENTAL SETUP

The experiment was performed in an apparatus chamber with 120 cm in diameter and 28.5 cm in height as shown in Fig. 1. The apparatus was modified from a class A evaporation pan and placed on a table. The center of the pan and the table under it were drilled and fitted with a PVC pipe drain of 5 cm diameter and 5 cm length. This drain was used to let water and sediment flow in the radial direction toward the center of the apparatus and down into the drainage tank under the table during operation.

In the preparation stage, the drain was closed with a plug, and an acrylic ring of 28 cm height was placed at the center. The ring had many small holes in it to allow water to pass through. Sand was gently filled between the ring and the edge of the apparatus to the design height and it formed a donut-like sediment layer. Then, water was gradually filled inside the ring and flowed into the sediment layer through the small holes until the sand was saturated and the water level reached the height of the layer. Based on the horizontal water surface, the saturated sand layer surface was delicately adjusted. After that, water was filled again to 17 cm depth from the chamber bed to complete the preparation stage.

Table 1 Experimental runs.

Run	Type	d_{50} (mm)	d_{10} (mm)	Thickness (cm)
A-1	Medium sand	0.49	0.30	10
A-2				10
A-3				5
B-1	Medium sand	0.30	0.12	10
B-2				10
B-3				5
C-1	Fine sand	0.18	0.07	10
C-2				10
C-3				5

Three sizes of industrial, sieved sand were used in this study as shown in Table 1. Their grain size distributions were analyzed using sieve analysis and a hydrometer test. The first two coarser sizes (sands A and B) were a non-cohesive, medium sand with medium diameters (d_{50}) of 0.49 and 0.30 mm, respectively. The last and smallest size (sand C) was fine sand with d_{50} of 0.18 mm and had a small proportion of silt and clay (~8% smaller than 62.5 μm) providing some cohesion. We conducted three experimental runs for each sand type. The first two runs were conducted under the same conditions using a layer thickness of 10 cm. The third run used a thickness of 5 cm. Thus, we performed a total of nine runs. Sand was not reused to ensure the same properties of sediment in each run.

Before the operation, the ring was removed very slowly to keep a symmetrical circular front of the sand layer at the center, and some debris floating on water surface was removed. A video camera was installed above the apparatus to record the evolution of the sand layer from the top view (Top Camera), and two video cameras were placed near the chamber edge to record the water levels at the two gauges attached to the inner edge (Cameras 1 and 2). When the set up was completed, the drain plug was opened. The video records ended when there was no further significant change in the sand layer. Two types of results were digitized from the records: the evolution of the sand layer crest from the Top Camera and the time variation of water levels at the gauges from Cameras 1 and 2.

3. RESULTS AND DISCUSSION

3.1 Geomorphological Processes

Figure 2 illustrates the general development observed during the experimental runs, which could be divided into three stages. Each experiment began when the center drain opened. In the beginning (Stage I), water on the sand layer was still deep. The whole water surface level descended almost horizontally similar to the case of pressurized flow through a drain from a large cylinder tank. The flow discharge was controlled by the height of the water level and the drain size. Due to the high water depth and restricted discharge, the flow velocity was very low and not sufficient to mobilize sand. Thus, no sediment transport was observed during this stage.

When the falling water level reached a certain level (approximately 1 cm above the sand layer level at the gauges), the water surface profile started to form a drawdown curve, and suddenly a very strong accelerating flow velocity toward the drain could be observed. In this Stage II, the flow velocity became strong enough to cause sediment entrainment in the vicinity of the crest. This fluvial erosion shaped a convex crest of sand layer and generated the expansion and upstream migration of the whole circular crest line. Mass wasting did not occur due to the high water level above the drain stabilizing the front slope in this stage. As the water level decreased further, the shallower flow could not erode the sand layer uniformly, and a number of incisions were initiated on the front. Some of them kept developing into main channels if they were able to tap water from an upstream area. Many rills with very small spacing were observed on the crest line when the water was very shallow in the later development.

As the water level fell well below the sand layer (Stage III), a large difference of water depths inside the sand layer and above the drain led to a high gradient of groundwater level and resulted in water emerging as seepage at the toe of the front. Seepage and the low water level destabilized the front and caused mass wasting. Mass wasting happened particularly at the section between two adjacent main channels where fluvial erosion had ceased. In the case of the cohesionless sands A and B, the common, complex combination of slope failure processes consisting of an upper slump motion and a transformed lower flow was detected. However, with sand C, cohesion allowed its sediment layer to resist erosion better than the others. Slow soil creep and earth flow were observed, and large-scale, slump block failure sometimes happened.

3.2 Channel Patterns

Figure 3 shows the top view of the final drainage networks from the Top Camera. The lines with dots show the digitized hole circumferences according to the uneroded crest lines of sand layers. Since water flowed in the radial direction and converged on the center drain of our circular apparatus, overall there was a centripetal drainage pattern. In every run, fluvial erosion (sheet and rill erosion) and mass wasting processes always occurred repeatedly and randomly in the vicinity of the crest and front of sand layers. Thus, incised channels were initiated at

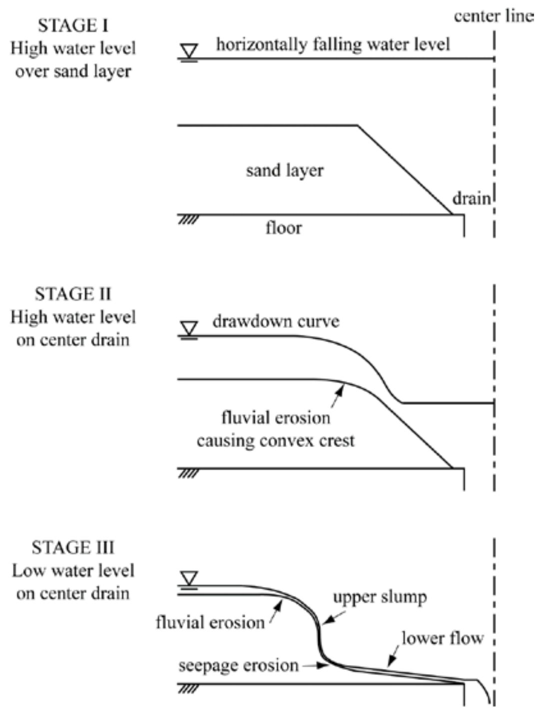

Fig. 2 Experiment setup.

the crests, where velocities are highest, and extended upstream. Because the experimental runs happened on short timescales, weathering processes such as abrasion did not affect our results, and, thus, we limited our consideration to the sand type and layer thickness, causing different channel patterns. It can be seen that the runs with sub numbers 1 and 2 of the same sand type have similar channel patterns. For the case of the runs with sub number 3, where the thickness was cut by half, less development of channel pattern was noticed. A shallower layer caused less seepage and mass wasting and also a milder slope of the front at the end. These induced less erosion and consequently shallower and shorter incised channels.

For sand A, short incised channels were observed with smaller rills in the eroded area. Several incised channels were able to tap the surface water from upstream and developed into longer main channels. In runs A-1 and A-2, long and steep cliffs with cavities at the toes were detected in the area where the overland flow stopped more rapidly than in other places and main channels were not found. The front subjected to seepage erosion can be divided into three zones [7]. The sapping zone is the small area near the toe where seepage emerges and the strong force of the effluent seepage initiates sediment detachment and removal from the face. Then, slope failure occurs in the undermining zone on top of the sapping zone due to losing its stability. Finally, sediment transported by fluvial processes in the fluvial zone downstream from the sapping zone

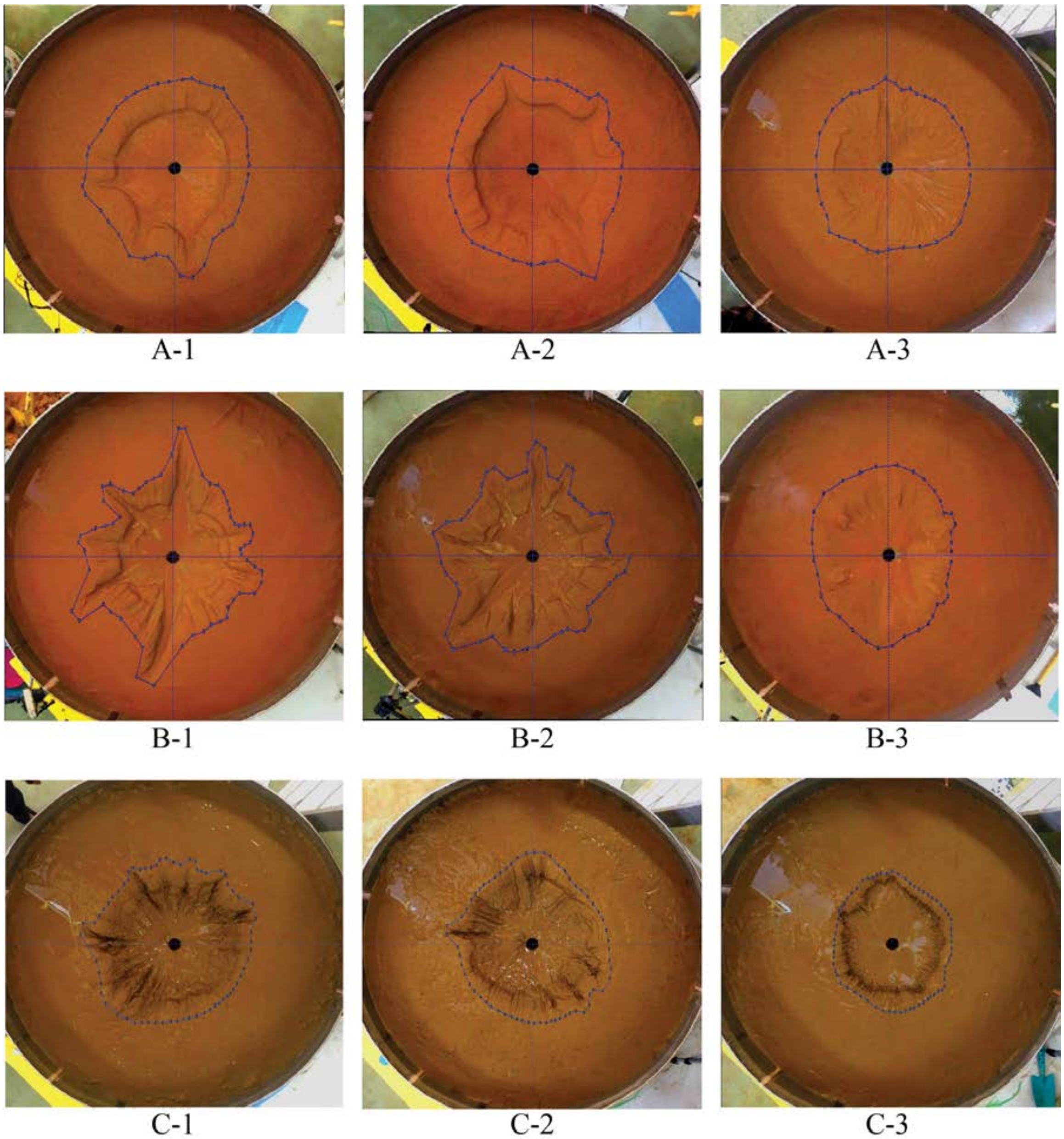

Fig. 3 Photographs of drainage networks in the final stage. Lines with dots show digitized hole circumferences.

helps a repeat of the processes. Thus, the cavities might be generated by seepage erosion in the sapping zone and surface tension between water and sand tends to hold the steep cliffs in the wet undermining zone. In run A-3, a not very long cliff was detected due to thinner thickness. The cavities were less in the experimental runs of sand B, and they were not found in sand C.

Compared with sand A, more main channels were observed in sand B, and they extended further upstream. Channel formation was very symmetrical in the radial direction. In addition, more small rills were also spotted caused by an increase in the strength of channel incision by overland flow because a smaller sediment size leads to lower threshold shear stress for erosion. Since a smaller diameter of sand B provides lower hydraulic conductivity corresponding to less infiltration, surface sheet flow erosion was stronger in the runs of sand B. Again, steep cliffs were detected in runs B-1 and B-2 due to seepage erosion and slump blocks, but it was not detected in run B-3 because of the lower height of the sand layer. Mass wasting is commonly assumed to be a diffusive-type process that smoothens topographic perturbations, while channel incision due to water flow amplifies perturbations. Thus, more extensive incised channels in sand B than in sand A were possibly the results of the stronger process of channel incision by overland flow related to mass wasting.

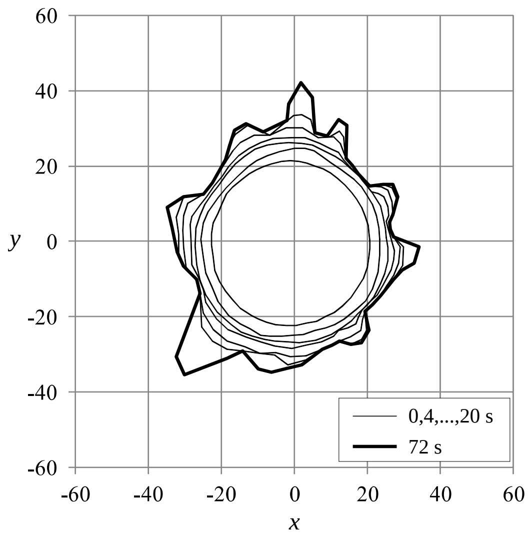

Fig. 4 Time variation in center hole circumference of run B-2.

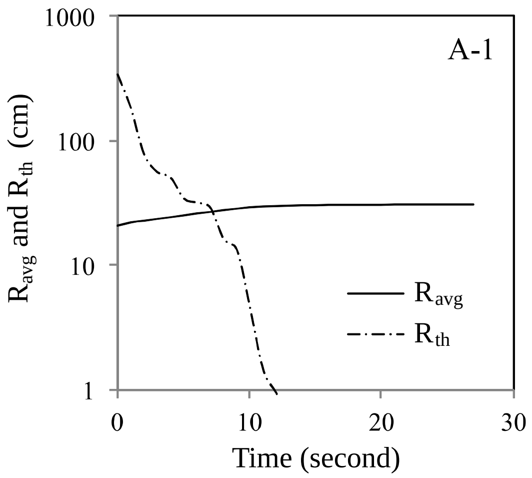

Fig. 5 Time series variations in average radius and threshold radius for run A-1.

Sand C contains a small percentage of mud. Due to having the smallest diameter and the presence of mud, the lowest hydraulic conductivity can be expected. Also, physical cohesion imparted by the mud can significantly influence and reduce the erosive properties of sediment. Many deep, incised rills of narrow width were found. In sand C, we did not observe steep cliffs with cavities as were found in sands A and B. However, soil creep and large-scale block slump were observed during the final stage of the runs when water at the drain had almost disappeared. The failure was possibly due to the low permeability of sand C so that it took a long time for water in the soil to drain. An increase in the soil weight due to the high water content without a counter-balance pressure force by the water level above the drain would be the main factor causing the large-scale failure. In addition, we observed a few step-like, upstream-migrating headcuts within some eroding channels by overland flow. However, they were decaying and finally disappeared as the surface water supplying their channel heads became weaker and finally ceased.

An example of the evolution of the center hole by digitizing sand layer crest lines is illustrated in Fig. 4. It shows the expansion of the hole circumference of the experimental run B-2 from 0 s to 20 s with two-second intervals, and at 72 s as the final pattern. The crest line is defined as the edge of the uneroded top surface of sand layer. We set time 0 when we first detected the start of erosion on the crest line. An initial, almost perfect circular circumference gradually developed into an irregular shape for the crest line due to the presence of main channels. At 72 s, we counted nine rounded corners from the digitized line, but the number of incised channels in the eroded area in the center photo of Fig. 3 was found to be greater than nine because some adjacent incised channels shared the same corner. Thus, the initiation of incised channels in the eroded area and the evolution of the crest line of the uneroded top surface may be generated by the same erosional process by overland flow and interact with each other, but their morphological processes and features can be different.

3.3 Analysis of Channel Head Evolution

At the commencement of drainage evolution in our experiment, the hole expanded while it still maintaining its circular shape. This implied that the hole was stable from perturbations. However, after expanding for a while, the hole became unstable and incised channels were initiated and grew upstream. Thus, there should be a threshold condition whereby an initially circular hole transforms into a channelized drainage.

To investigate the threshold condition, we adopted the recent linear stability analysis [3]. We calculated the threshold channel head radius for channelization (R_{th}) and compare it with the experimental average radius (R_{avg}) for every 1 second interval. Figure 5 shows the time series variations in both radii for Run A-1. It was found that an initial (R_{avg}) was smaller than an initial R_{th}. The initial R_{avg} was around 20 cm while the initial R_{th} was much larger in the order of several hundred centimeters. However, as time progressed, R_{avg} increased slowly while R_{th} decreased rapidly due to decreasing discharge. At around t = 7 s, R_{avg} = R_{th}, which implied that channelization could take place. In every experiment, a similar trend was found although the time of the intersection between R_{avg}

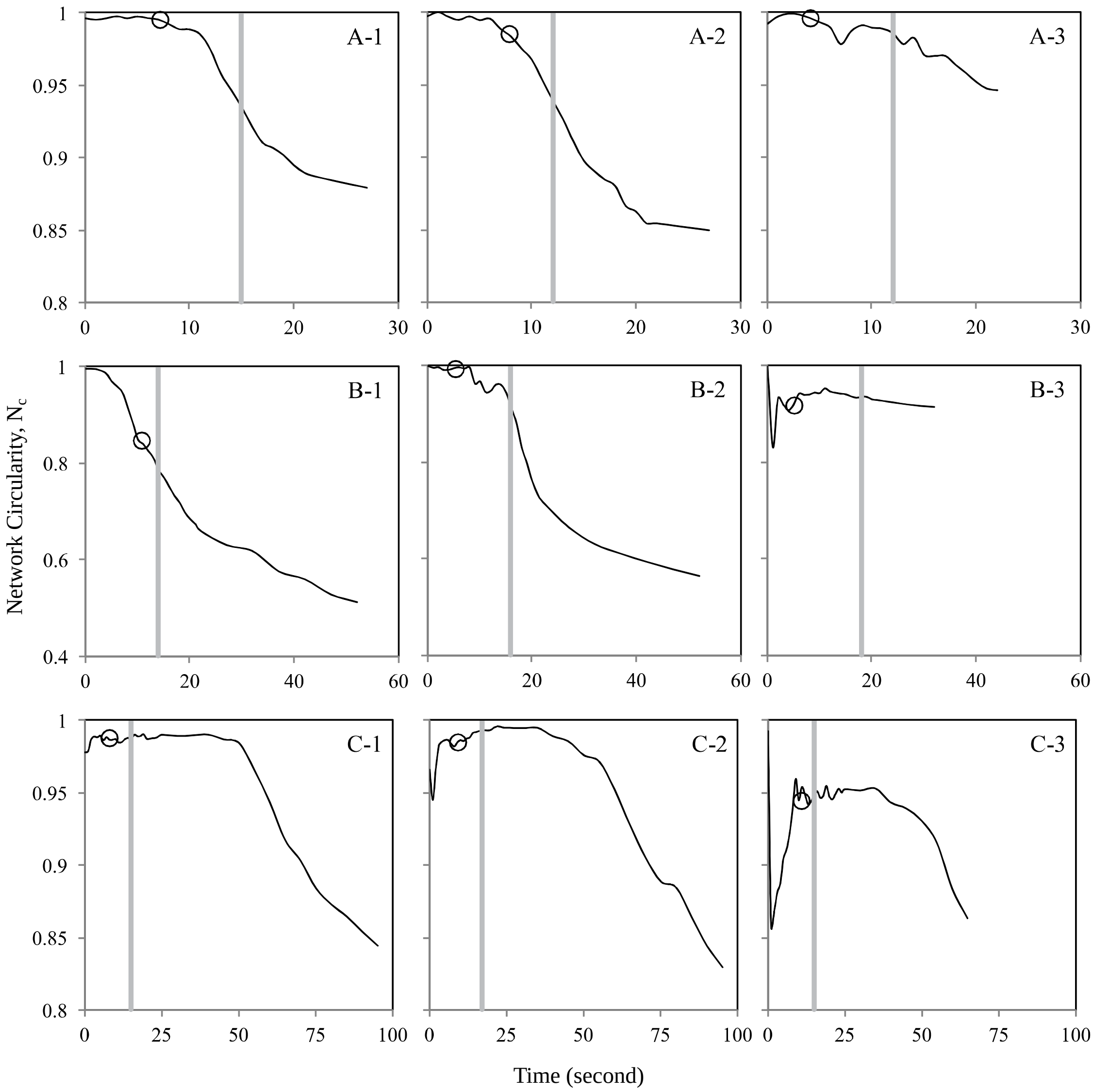

Fig. 6 Time series variations in network circularity. Shaded vertical lines show predicted time of no uniform sheet surface flow, and circles show time of bifurcation predicted by the theory [3].

and R_{th} varied.

Gomez and Mullen [8] performed an experiment on channel networks by considering groundwater flow. To describe the shape of their experimental drainage networks, they adopted the concept of circularity by [9] that has been used to quantify the shape of a whole drainage basin. They called it network circularity (N_c) defined as the ratio between the eroded network area and the circle area of the same perimeter as follows:

$$N_c = A/A_c = A/\pi(P/2\pi)^2 \quad (1)$$

where A and P are the eroded area and perimeter of channel network, respectively, and A_c is the circle area computed using P.

Network circularity N_c has a value between 0 and 1 where N_c = 1 means that the shape of the channel network is perfectly circular. Using N_c, three phases of channel network development was proposed as follows [8]. (1) Initiation is the first stage during which the main channels elongate upstream rapidly. N_c decreases steeply in this stage. (2) Extension is the second stage in which the channel heads expand laterally and bifurcate into tributary channels. N_c still continues reducing but at a lower rate. (3) Abstraction is the last stage in which the channel heads continue widening and cause divide decay and consequently P may reduce while A still increases. N_c thus begins to increase.

Figure 6 shows the variation in network circularity with time for every run. In general, the initial N_c was close to unity and remained so for

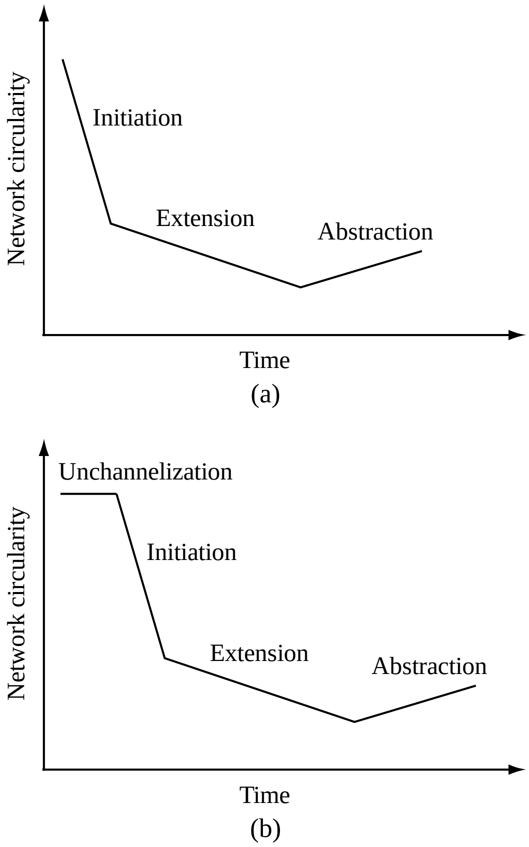

Fig. 7 Phases of network evolution classified by network circularity (a) proposed by [8] and (b) by this study to include unchannelization phase.

some period before reducing rapidly. With sands A and B, the reduction in N_c occurred before the uniform overland flow had disappeared, while for sand C, it occurred after that and took quite a long time of about 1 min. As the sand size decreased, evolution took longer. In run C-2, during the beginning period, N_c abruptly dropped and then regained because there were small, initial, irregular perturbations along the crest line before the operation. The perturbations disappeared later because the eroding crest neighboring them migrated upstream at a faster rate, and thus the crest lines around the perturbations became rounder and wider. This implied that the network dynamics favored maintaining a circular shape. If we assume that channel inception can be indicated by the slope transition of N_c, it can be said that in the cases of sands A and B, channelization took place during active, uniform overland flow while it happened later with sand C. Comparing the slope transition with the prediction by the theory shown in circles, we found qualitative agreement for sands A and B. Due to the largest threshold erosion of sand C, it was possible that the active erosion time was too short to generate channelization during the uniform overland flow period. The channelization in runs using sand C was due to some incised channels being able to tap water from depressions on the layer surface.

In the phases of network evolution proposed by [8] as shown in Fig. 7a, the first phase in our experiment where the network circularity N_c maintained its value cannot be explained. However, this phase was detected in other experiments. Hancock and Willgoose [10] studied network development in a landscape simulator. They described the first phase in their experiment where surface water flowed to and concentrated at the basin outlet, and it caused the expansion of an unchannelized, large, semi-circular eroded area. Channelization then took place at this eroded area and the channel network developed from there upstream in later phases. This first phase was also found in the experiment of [11]. Thus, we proposed to include this phase of the development of unchannelized area into the original phase diagram. Figure 7b shows the revised phases of network evolution. The first phase, where the shape of eroded area remains or N_c keeps constant, was added and was called the “unchannelization” phase.

4. CONCLUSION

The experiment of channel bifurcation on a circular hole was performed with three sand diameters (d_{50} = 0.49, 0.30 and 0.18 mm) and two layer heights (10 and 5 cm). The smallest size had a small proportion of silt and clay and showed the presence of cohesion and the lowest erodibility. In the runs of the two largest sizes, the combination of slope failure processes of an upper slump motion and a transformed lower flow was observed. However, slow soil creep and earth flow with large-scale slump block failure were found in the case of the smallest size due to cohesion, and step-like upstream-migrating headcuts (cyclic steps) were also detected during the runs. Seepage and seepage erosion were strongest for the largest size due to the highest hydraulic conductivity. The middle-sized sand showed the greatest extension of channelization with radial symmetry due to high erodibility.

According to [8], network evolution can be divided into three phases (initiation, extension and abstraction). The initiation phase was the first phase of the evolution when main channels elongate rapidly. However, from our experimental runs, circular holes were not incised by main channels unless the hole radii were sufficiently large compared with the flow discharge. Thus, we proposed a new first phase called the unchannelization phase where the shape of the eroded area remains unchanged. The transition between the unchannelization phase and the initiation phase is then expected to be the time of incipient channelization according to the theory by [3].

The latest experimental, numerical and theoretical studies [12]-[14] show that bifurcation generated by overland flow and seepage erosion should be investigated by process-based approaches. Thus, better flow models and erosion functions may be necessary and important for future research.

5. ACKNOWLEDGMENTS

The authors would like to thank Mr. Wirot Sriaut for helping set up the experiment and Prof. Dr. Suched Likitlersuang for support in the soil testing laboratory. The first author was supported by the Japan Society for the Promotion of Science Invitation Fellowship Program (grant-in-aid L-14542) and the Kasetsart University Research and Development Institute (KURDI).

6. REFERENCES

[1] Perron, J. T., P. W. Richardson, K. L. Ferrier, and M. Lapoôtre, The root of branching river networks, Nature, 492, 2012, pp.100-103.

[2] Petroff, A. P., O. Devauchelle, H. Seybold, and D. H. Rothman, Bifurcation dynamics of natural drainage networks, Philosophical Transactions of the Royal Society A: Mathematical, Physical and Engineering Sciences, 371(2004), 2013, pp.20120365..

[3] Pornprommin, A., N. Izumi, and G. Parker, Initiation of channel head bifurcation by overland flow, Journal of Geophysical Research: Earth Surface, 122(12), 2017, pp.2348-2369.

[4] Pornprommin, A., Y. Takei, A. M. Wubneh, and N. Izumi, Channel inception in cohesionless sediment by seepage erosion, Journal of Hydro-environment Research, 3(4), 2010, pp.232-238.

[5] Berhanu, M., A. Petroff, O. Devauchelle, A. Kudrolli, and D. H. Rothman, Shape and dynamics of seepage erosion in a horizontal granular bed, Physical Review E, 86(4), 2012, pp.041304.

[6] Marra, W. A., S. J. McLelland, D. R. Parsons, B. J. Murphy, E. Hauber, and M. G. Kleinhans, Groundwater seepage landscapes from distant and local sources in experiments and on Mars, Earth Surface Dynamics, 3(3), 2015, pp.389-408

[7] Howard, A. D., and C. F. McLane III, Erosion of cohesionless sediment by ground water seepage, Water Resources Research, 24(10), 1988, pp.1659-1674.

[8] Gomez, B., and V. T. Mullen, An experimental study of sapped drainage network development, Earth Surface Processes and Landforms, 17(5), 1992, pp.465-476.

[9] Miller, V. C., A quantitative geomorphic study of drainage basin characteristics in the Clinch Mountain area, Virginia and Tennessee, Columbia University Technical Report 3, Project NR 389-042, 1953, 68 pp., New York.

[10] Hancock, G., and G. Willgoose, The interaction between hydrology and geomorphology in a landscape simulator experiment, Hydrological Processes, 15(1), 2001, pp.115-133.

[11] Brasington, J., and R. M. A. Smart, Close range digital photogrammetric analysis of experimental drainage basin evolution, Earth Surface Processes and Landforms, 28(3), 2003, pp.231-247.

[12] Thaisiam, W., P. Kaewnon, and A. Pornprommin, Experiment of channelization due to seepage erosion, International Journal of GEOMATE, 14(46), 2018, pp.137-142.

[13] Sutidhanakul, T., W. Thaisiam, and A. Pornprommin, Groundwater Flow Simulation to Analyze Channel Head Bifurcation, Journal of King Mongkut's University of Technology North Bangkok, 29(1), 2019, pp.14-22.

[14] Smith, T. R., Analytic theory of equilibrium fluvial landscapes: The integration of hillslopes and channels, Journal of Geophysical Research: Earth Surface, 123(3), 2018, pp.557-615.